

Transfer of displacement from multiple slip zones to a major detachment in an extensional regime: Example from the Dead Sea rift, Israel

Michael R. Gross*

Department of Geology, Florida International University, Miami, Florida 33199

Alexander Becker

Ramon Science Center, Jacob Blaustein Institute for Desert Research, Ben-Gurion University of the Negev, P.O. Box 194, Mizpe Ramon 80600, Israel

Gabriel Gutiérrez-Alonso

Departamento de Geología, Universidad de Salamanca, 37008 Salamanca, Spain

ABSTRACT

Fabric development and block rotation related to flexural slip were examined in sedimentary strata draped over a basement normal fault at the western margin of the Dead Sea rift in southern Israel. In addition to documenting differences in deformation style as a function of lithology, this study focuses on the progressive development of flexural-slip horizons and fabric development in extensional settings. Deformation in the intercalated shale, siltstone, carbonate, and gypsum beds of the Turonian Ora Formation is dominated by extension, bedding-plane slip, and block rotation, which occur at different scales and magnitudes throughout the approximately 12 m section. Extension appears as boudinage in carbonate beds and fibrous sigmoidal gypsum veins in shale, whereas strong foliation, highly deformed gypsum veins, and asymmetric folds characterize slip and adjacent drag zones. Magnitude of extension in individual beds is directly related to relative magnitude of adjacent bedding-plane-slip horizons, implying a common origin. Initial flexural slip was lithologically controlled, with displacement occurring along numerous narrow zones throughout shale and siltstone horizons. Continued top-to-the-west bedding-plane slip, however, led to antithetic block rotation within competent beds, which in turn resulted in the termination of slip along zones abutting block-bounding faults. As block size increased during progressive development of flexural slip, so did the spacing between active slip zones. Therefore, rigid block rotation within subhorizontal simple shear zones provided the mechanism for concentrating flexural slip along several major detachments during extension of the Ora Formation above a basin-bounding normal fault.

INTRODUCTION

Abundant oil and gas production from regions such as the Gulf of Mexico, North Sea, and the Gulf of Suez demonstrates that significant deposits of fossil fuels are found in extensional tectonic settings. Although the geometries and development of normal fault systems have been studied in detail (e.g., Wernicke and Burchfiel, 1982; Jackson and McKenzie, 1983; Etheridge et al., 1985; Lister et al., 1986; Gibbs, 1987; Roberts and Yielding, 1994; Schlische, 1995), numerous aspects of structural development in extensional regimes remain unresolved. One process that has received little

attention in terms of extensional faulting and folding is the mechanism of flexural slip, which typically occurs in rocks composed of heterogeneous lithologies. Flexural slip, in turn, can lead to the development of unique structures that may effectively trap and seal hydrocarbons, thus providing potential targets for oil and gas exploration.

Flexural slip is the dominant mechanism for accommodating upper crustal folding in sequences of layered sedimentary rocks that display large competence contrasts (e.g., Ramsay, 1967, 1974; Chapple and Spang, 1974; Behzadi and Dubey, 1980; Tanner, 1989; Alonso, 1989; Becker et al., 1995). Slip typically occurs along bed boundaries or within more ductile strata and increases in magnitude from zero at the fold hinge to a maximum along the limbs. If the fold is circular with limbs dipping less than 70°, then the magnitude of slip is linearly proportional to limb dip and to the thickness of strata between slip horizons (Suppe, 1985). Whereas flexural slip has been widely reported for folds in contractional settings, this mechanism has not been thoroughly documented in regions subjected to extension. A sketch depicting sedimentary layers draped over a basement normal fault shows how flexural slip can develop in an extensional environment (Fig. 1). In this example of a monocline, flexural slip displays a consistent top-to-the-left sense of displacement; maximum displacement occurs in the region of

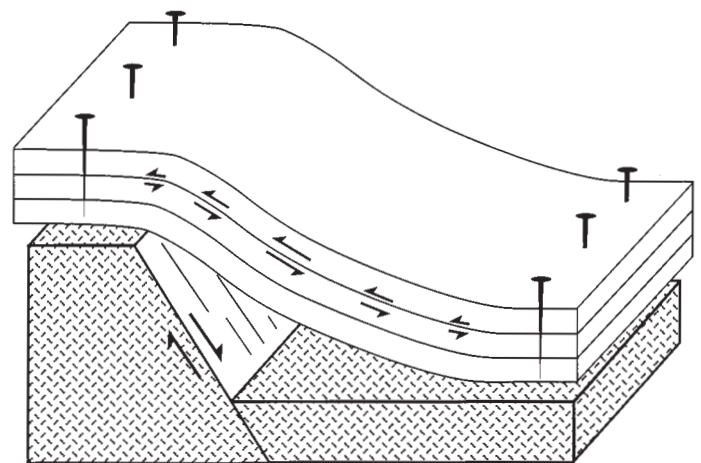


Figure 1. Direction and relative amount of flexural slip in a draped monocline developed above a basement normal fault. The flexural-slip mechanism results in simple shear parallel to bedding.

*E-mail: grossm@servax.fiu.edu

steepest dip, and decreases to zero where beds are horizontal. In a study of flexural-slip folding in turbidite sequences subjected to tectonic contraction, Tanner (1989) identified thin, fibrous, lineated, bedding-parallel quartz veins as key horizons that accommodate displacement during folding. Tanner (1992) also described the development of flexural-slip duplexes with floor and roof thrusts in steep limbs of folds.

Descriptions of fabrics that develop in extensional settings, especially those related to flexural slip, are not abundant in the geologic literature. Structures and internal fabrics most commonly associated with extension are veins (e.g., Ramsay and Huber, 1987), boudinage (e.g., Ramberg, 1955; Gaudemer and Tapponnier, 1987; Malavieille, 1987; Goldstein, 1988), extensional crenulation cleavage (Platt, 1979, 1984; Platt and Vissers, 1980), and antithetically rotated asymmetric pull-aparts (Hanmer, 1986; Jackson et al., 1988; Jordan, 1991). The latter structures, also referred to as extensional or asymmetric shear bands (Marcoux et al., 1987; Stock, 1992), are a series of blocks that rotate between slip horizons as a result of layer-parallel stretching. The sense of rotation for antithetic pull-aparts in simple shear zones is opposite to that for domino or bookshelf structures (Fig. 2).

In this paper we investigate the development of internal fabrics and block rotations within a heterogeneous sedimentary sequence on the margin of the Dead Sea rift valley. We describe the mechanism of flexural-slip folding as it applies to a fault-related monocline that formed under regional extension, as well as the fabrics and mesoscopic structures that developed during this process. In addition, we demonstrate how bedding-plane slip, initially distributed across many lithologically controlled horizons, becomes concentrated along several major detachments due to rigid block rotation around subhorizontal axes.

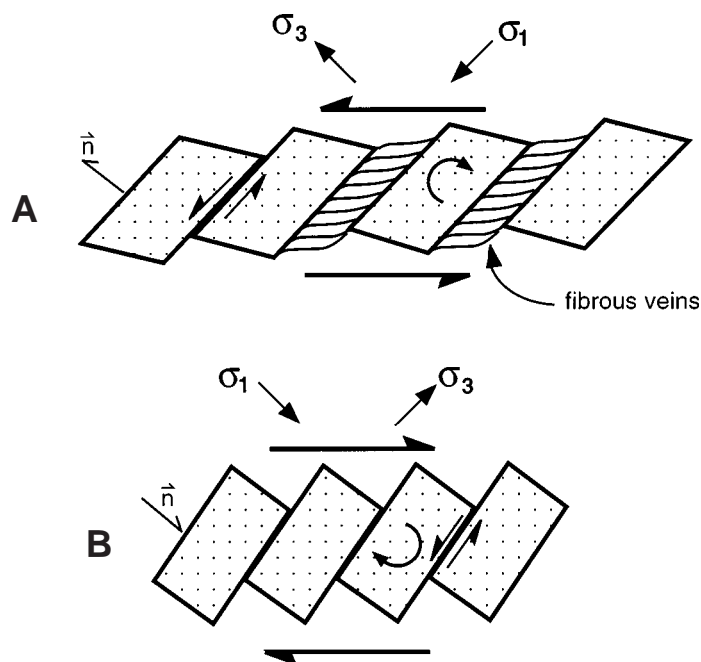


Figure 2. (A) Antithetically rotated asymmetric pull-aparts and (B) synthetically rotated domino or bookshelf structures (adapted from Jordan, 1991). Note how similar geometries may result from opposing shear senses. The difference is that antithetically rotated blocks develop under layer-parallel extension and layer-normal contraction. Extensional vein material commonly forms between blocks due to the large component of σ_3 normal to block-bounding faults (n is the normal to the fault surface).

GEOLOGIC SETTING

The outcrop selected for analysis is a section of shallow-marine sedimentary rocks exposed continuously for more than 270 m, located in southern Israel at the western margin of the Dead Sea rift valley, about 60 km north of the Gulf of Elat (Fig. 3A). Basin-bounding normal faults and other extensional features are commonly found along the margins of the Dead Sea rift (e.g., Quennel, 1959; Zak and Freund, 1966; Eyal, 1973; Garfunkel, 1981; Garfunkel et al., 1981; Arkin, 1989; Ginat, 1995). The combination of diverse lithology, variety of deformation structures, abundance of kinematic indicators, and unique position with respect to the Dead Sea rift provide an outstanding opportunity to investigate the mechanism of flexural slip in an extensional tectonic setting.

The Ma'aleh Gerofit exposure is situated on the east-dipping limb of a structure that originated as a monoclin flexure above a down-dropped eastern basement block (Fig. 3B), and thus may be classified as a "drape" or "forced" fold (e.g., Stearns, 1978; Stone, 1993). The strata strike N10°W and dip approximately 20° to the east, and terminate to the east against a basin-bounding normal fault. Several large west-northwest-dipping normal faults are found in the central part of the outcrop (Figs. 4 and 5). The tops of these faults terminate against a major bedding-parallel detachment zone situated midway up the escarpment.

The lower part of the outcrop consists of intercalated shale, gypsum, and dolostone beds belonging to the lower Turonian Ora Formation, which has a total thickness of approximately 110 m (Bartov et al., 1972; Ginat, 1995). These beds display a wide range of colors, which provide excellent marker horizons for measuring displacements and observing detachment horizons. The Ora Formation is underlain by massive limestone and dolostone beds of the Hazera Formation (Albian-Cenomanian, 140 m; Lewy, 1988) and overlain by the upper Turonian limestone of the Gerofit Formation (160 m; Bartov et al., 1972; Ginat, 1995; Fig. 3C). Although the Hazera Formation is not exposed at the study site, the base of the Gerofit Formation appears in the upper part of the outcrop. The incompetent shale and gypsum layers of the Ora Formation occupy a key position between two massive carbonate units, and thus the Ora Formation is a prime candidate for accommodating flexural slip within this stratigraphic interval. Our study is restricted to an interval approximately 12 m thick in the Ora Formation between the base of the outcrop and the thick black shale unit in contact with the base of the Gerofit Formation.

KINEMATIC INDICATORS

Kinematic indicators observed in the Ma'aleh Gerofit section include sigmoidal gypsum veins, asymmetric folds, offset vertical veins, and microstructural fabrics.

Sigmoidal Gypsum Veins

The most prominent deformation feature observed in outcrop are sigmoidal gypsum veins, which range in length from several centimeters to several meters. Veins appear either as individual sigmoids, with thick oblique middle sections pinching out in thin tails parallel to bedding (Fig. 6A), or as an array of en echelon sigmoids that merge into a common bedding-parallel vein (Fig. 6B).

Two observations indicate that sigmoidal veins originated oblique to bedding, and subsequently utilized planes of weakness along shale partings to assume bedding-parallel geometries. First, oblique and bed-parallel veins do not crosscut each other, but rather gypsum fibers demonstrate continuity of growth from oblique to bed-parallel veins. Second, the continuity of bedding-parallel gypsum veins depends upon the development of individual sigmoidal veins; in areas where sigmoidal veins are poorly developed, ad-

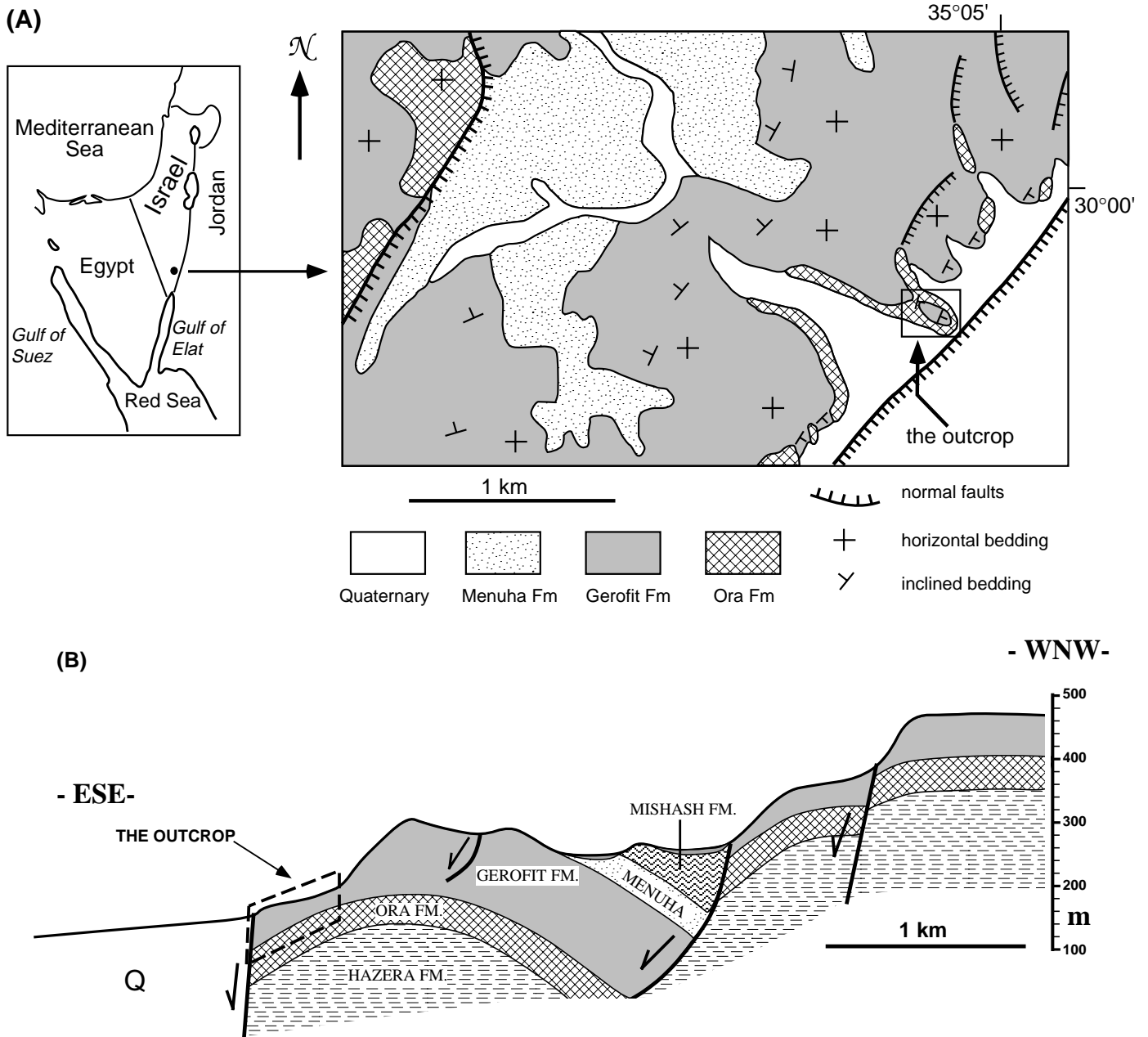


Figure 3. (A) Outcrop location and geologic map (after Ginat, 1995); (B) Cross section through Ma'aleh Gerofit Pass.

adjacent bedding-parallel veins are discontinuous. Initial sigmoidal vein shape and an echelon alignment result from curved fracture growth rather than bridge rotation, because local bedding within intervening shale wall rock remains aligned parallel to overall bedding.

The overwhelming majority of sigmoidal gypsum veins dip consistently to the west, although thin, east-dipping sigmoids are found in several isolated mechanical units ("mechanical unit" is defined as a rock unit that exhibits a specific style of deformation). Principal stress orientations that prevailed during sigmoidal vein development within parallel shear zones are shown schematically in Figure 7; σ_3 is normal to the planar central part of the sigmoid, σ_2 is parallel to the axis of curvature, and σ_1 is in the plane of the central part and normal to the curvature axis.

Asymmetric Folds

A second group of kinematic indicators observed in the Ora Formation consists of asymmetric folds, which appear in the form of curved siltstone and shale bedding traces or folded bedding-parallel gypsum veins of tectonic origin (Fig. 6C). The asymmetry, and hence sense of vergence of folded gypsum veins, is unambiguous; the veins have short forelimbs, long backlimbs, and a few floating hinges (Fig. 6D). Folding is disharmonic and confined to shale and siltstone beds; folds are in sharp contact with adjacent unfolded mechanical units, and typically display tightly closed limbs. Veins folded in a similar manner were also reported by Hamner (1982).

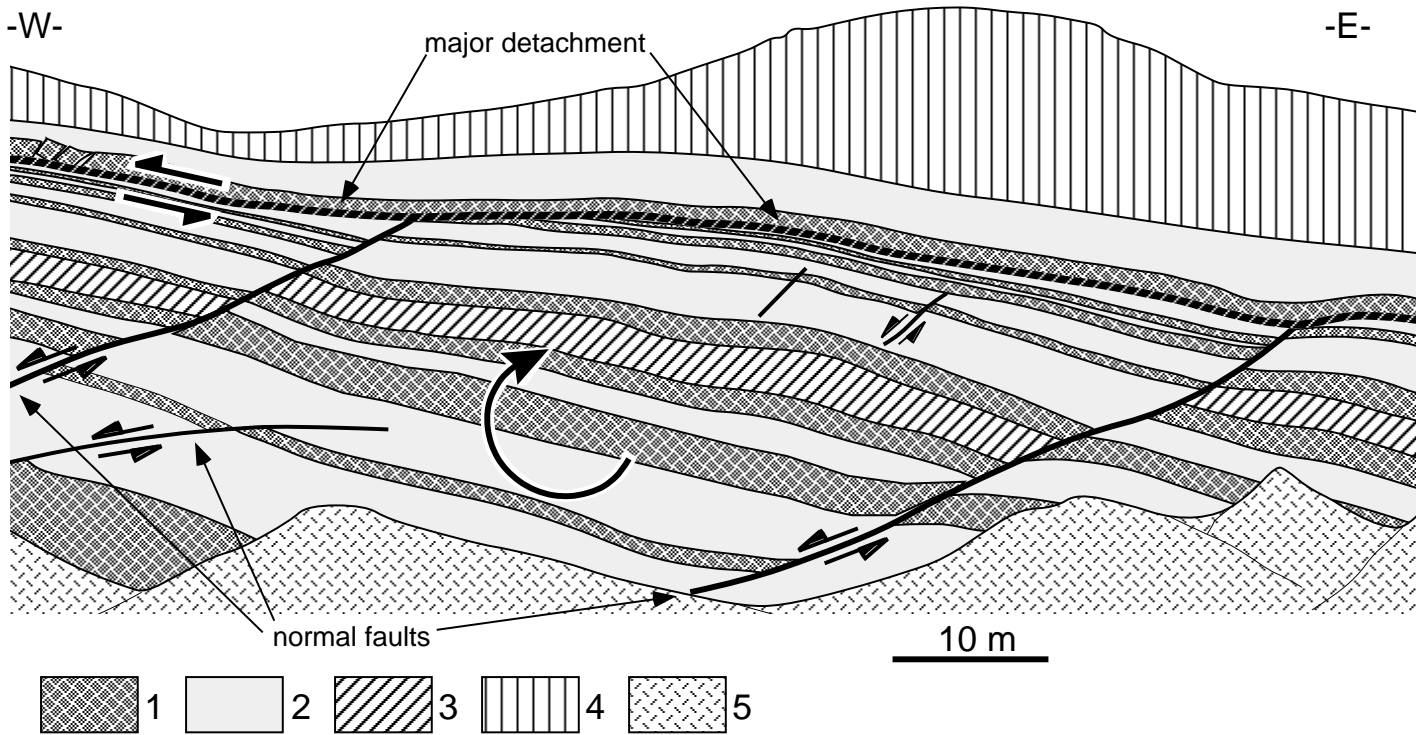


Figure 4. Outcrop sketch of major structural elements drawn from the photograph in Figure 5A. Ora Formation (1–3); 1—competent gypsum, dolostone, and limestone beds, 2—incompetent shale and siltstone beds, 3—shale bed containing large sigmoidal gypsum veins. Gerofit Formation; 4—limestone and dolomite. Talus—5. Circular arrow indicates sense of rotation for fault-bounded blocks.

Offset Vertical Veins

Several thin vertical gypsum veins are offset by bedding-plane faults, and thus provide additional kinematic criteria. Tanner (1989) used offset bedding-normal sedimentary dikes in similar fashion to document flexural slip in turbidite sequences. In the Ma’aleh Gerofit section, however, crosscutting relationships show that vertical veins are relatively late features that postdate initiation of bedding-plane slip. In addition, because vertical veins may propagate more easily across thin detachment horizons (i.e., they terminate against thicker slip zones), offsets are mostly observed across thin bedding-parallel faults. Therefore, the amount of slip determined from offset vertical veins rep-

resents a minimum value of displacement. Thin vertical veins display consistent top-to-the-west offset; displacements range from several millimeters to several centimeters.

Antithetically Rotated Asymmetric Pull-Aparts

Rotated rigid blocks, referred to as antithetically rotated asymmetric pull-aparts (Hanmer, 1986; Jordan, 1991), serve as an additional mesoscopic kinematic indicator. These blocks are termed “antithetic” because, with respect to the same simple shear couple, their sense of rotation is opposite to bookshelf structures (Fig. 2). They are considered ambiguous kinematic in-

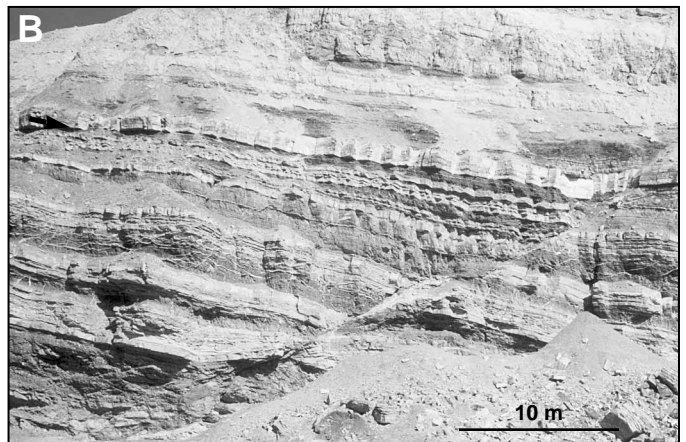


Figure 5. (A) Central part of outcrop; (B) closer view of outcrop showing offset across west-dipping normal fault. Arrow points to major bed-parallel detachment zone that acts as upper slip horizon for large rotating blocks.

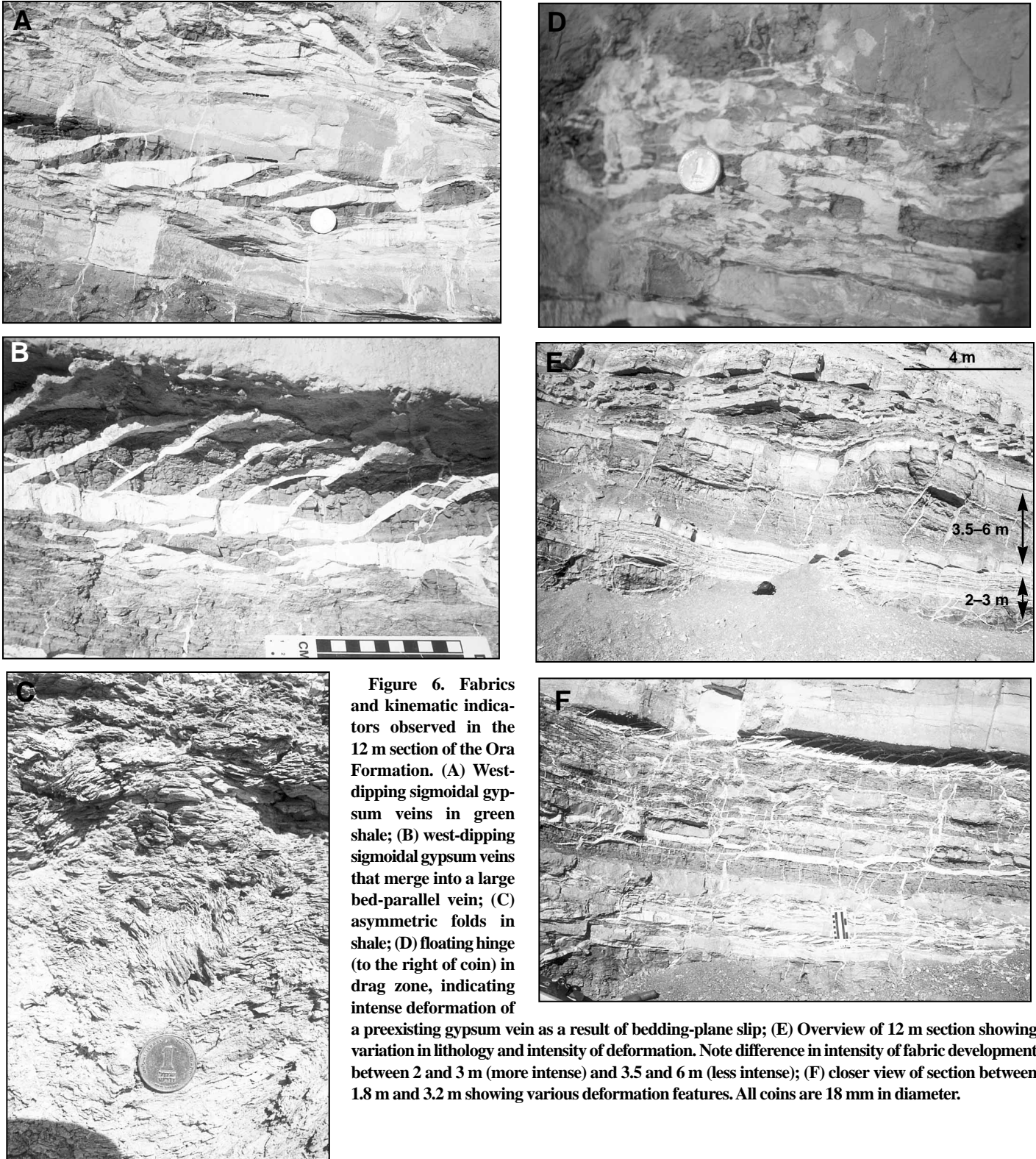


Figure 6. Fabrics and kinematic indicators observed in the 12 m section of the Ora Formation. (A) West-dipping sigmoidal gypsum veins in green shale; (B) west-dipping sigmoidal gypsum veins that merge into a large bed-parallel vein; (C) asymmetric folds in shale; (D) floating hinge (to the right of coin) in drag zone, indicating intense deformation of a preexisting gypsum vein as a result of bedding-plane slip; (E) Overview of 12 m section showing variation in lithology and intensity of deformation. Note difference in intensity of fabric development between 2 and 3 m (more intense) and 3.5 and 6 m (less intense); (F) closer view of section between 1.8 m and 3.2 m showing various deformation features. All coins are 18 mm in diameter.

indicators due to their possible synthetic or antithetic origin. One characteristic that strongly implies an antithetic origin, however, is the precipitation of extensional vein material between rotated blocks as gaps develop during layer-parallel stretching. Such gaps, commonly observed between rotated

blocks at the Ma'aleh Gerofit outcrop, do not develop during synthetic block rotation due to the resolved compressive normal stress acting across the block-bounding faults (Fig. 2).

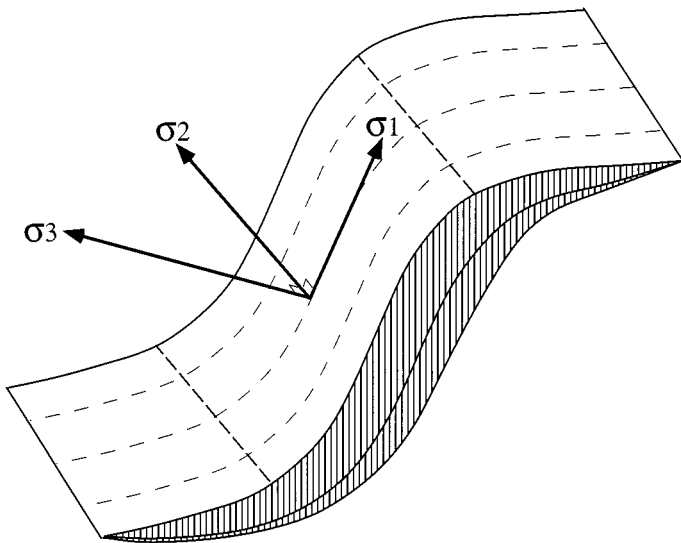


Figure 7. Orientation of principal stress axes during formation of sigmoidal gypsum veins: σ_3 is normal to planar central part of the vein; σ_2 lies in vein surface parallel to hinge line marking tail curvature; and σ_1 lies in planar central part, mutually perpendicular to σ_2 and σ_3 .

Microstructures

Many of the structures observed in outcrop appear in thin section, including gentle to isoclinal folds with disrupted or floating hinges, sigmoidal gypsum veins, brecciated zones parallel to bedding, and the folding of shale foliation. Folded gypsum veins in thin section display pronounced asymmetries; i.e., shortened forelimbs and extended and commonly fragmented backlimbs. Microfolds are typically outlined by thin horizons rich in silt-sized quartz particles, and tight chevron folds are found in conjunction with crenulated foliation in clay-rich horizons.

Orientation of Kinematic Indicators

Orientations of structural features measured in the Ma'aleh Gerofit outcrop, along with principal stresses derived from west-dipping sigmoidal veins, exhibit several noteworthy relationships (Fig. 8). First, sigmoidal gypsum veins and asymmetric fold hinges both reflect the same kinematic simple shear regime, as seen by the clustering of fold hinges around the σ_2 axis. Second, the calculated maximum principal stress plunges 33° to 274° , which when applied to the 349° , 16° E oriented strata, results in simple shear with top-to-the-west sense of motion. Third, the normal faults generally cluster into one group with a mean orientation of 201° , 64° NW. Conjugate normal fault pairs imply a pure shear origin, whereas one dominant normal fault population typically develops under simple shear conditions. Furthermore, that poles to normal faults lie in the σ_1 - σ_3 plane is entirely consistent with the top-to-the-west simple shear regime that resulted in the formation of sigmoidal veins and asymmetric folds. Therefore, upon analyzing the variety of kinematic indicators found at Ma'aleh Gerofit, a consistent top-to-the-west sense of motion emerges.

MECHANICAL STRATIGRAPHY

We measured and described mechanical stratigraphy at the Ma'aleh Gerofit outcrop for a section about 12 m in thickness, noting such features as lithology, intensity and style of deformation, and fabric development

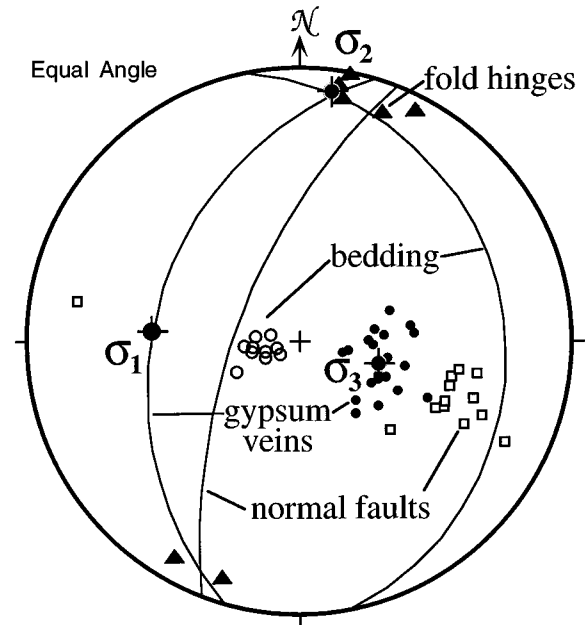


Figure 8. Lower hemisphere, equal-angle projection of kinematic indicators observed in the section, demonstrating top-to-the-west sense of slip. Structural elements and number of measurements include bedding (11), normal faults (13), sigmoidal gypsum veins (21), and hinges of folded gypsum veins (7).

(Figs. 6E, 6F, 9, 10). We use the term “mechanical stratigraphy” (Gross, 1995) to emphasize the point that style and intensity of deformation is highly variable, dividing the section into discrete horizons of deformation that do not necessarily correspond to lithologic or stratigraphic boundaries. We measured 74 mechanical units at Ma'aleh Gerofit, and each is distinguished on the basis of lithology and/or style of deformation.

Most of the section (approximately 70%) consists of shale and siltstone; bed thicknesses range from 0.5 to 190 cm. Shale and siltstone play key mechanical roles, because without exception all slip zones occur in these rock types. Bedded gypsum layers attain thicknesses up to 86 cm and are fragmented into joint-bounded rotated blocks that affect initial stages of flexural slip. Dolostone occurs as thin to medium horizons (1.2–28 cm in thickness) typically embedded in thicker shale layers. In general the type of fabric development is related to lithology; there are boudins or joints in carbonate rocks, joints in bedded gypsum, and sigmoidal veins, asymmetric folds, and foliation in shale and siltstone. The intensity of deformation varies widely throughout the section, so that highly deformed horizons may be found in contact with lightly deformed beds (Fig. 9). The zoning of flexural slip is characterized by discrete horizons that exhibit slip, drag, and extension, as described in the following sections.

Slip Zones

Zones of flexural slip display strong planar foliation parallel to bedding, and are present in shale and siltstone horizons at various positions in the section. Slip zones may occupy the entire shale horizon (e.g., 3.4 m and 6.35 m in the section), or occur as narrow zones of intense deformation within relatively undeformed shale (e.g., 2.3 m and 2.75 m in the section). Small (<0.5 cm in diameter) rounded particles of ground gypsum veins are commonly found within slip horizons (Fig. 11); the amount of ground gypsum increases toward the margins as slip zones widen to incorporate material from adjacent drag zones.

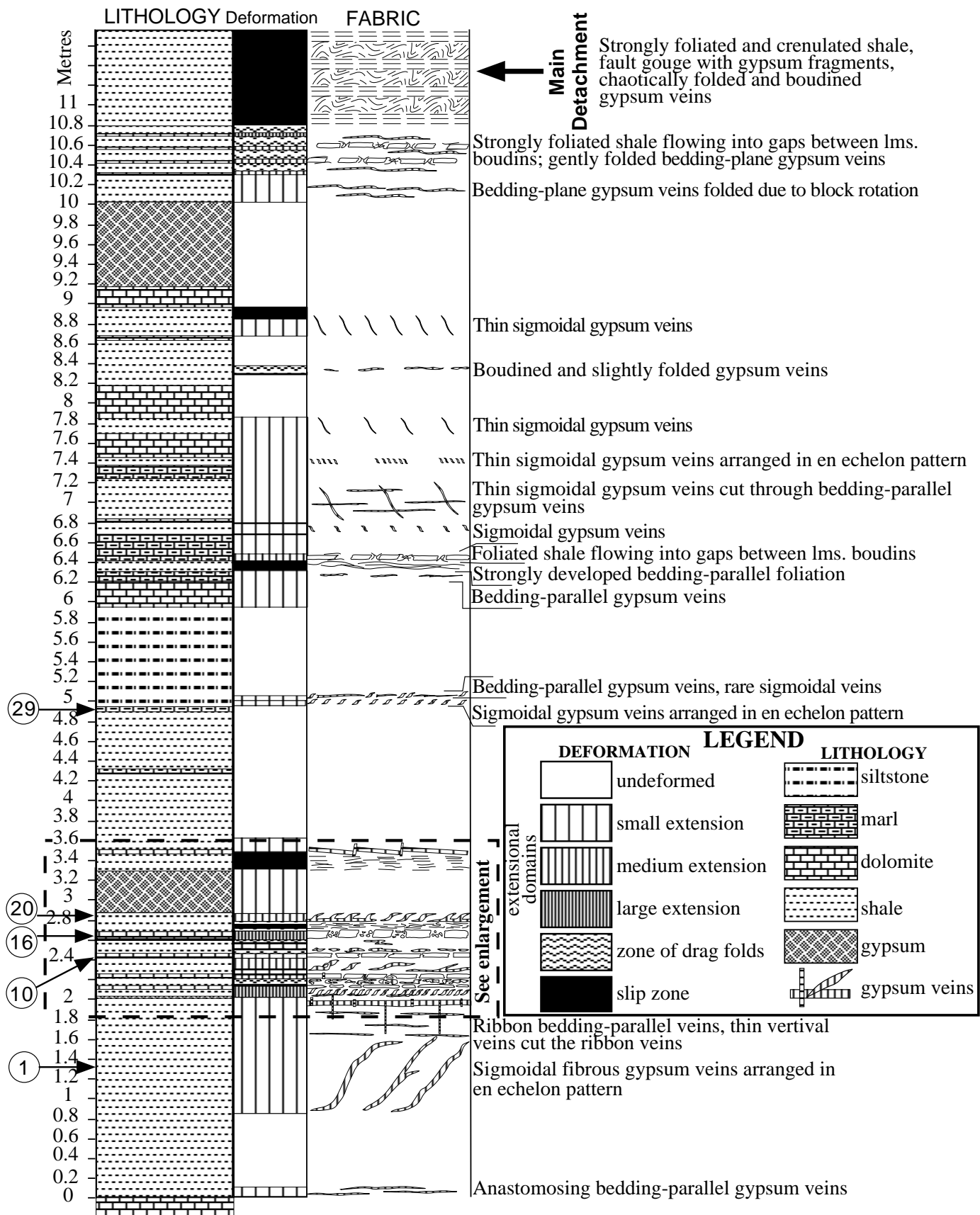


Figure 9. Mechanical stratigraphy of the Ma'aleh Gerofit section, including lithology, intensity of deformation, fabric, and brief description. Arrows left of column indicate locations of mechanical units where extensional strain was measured.

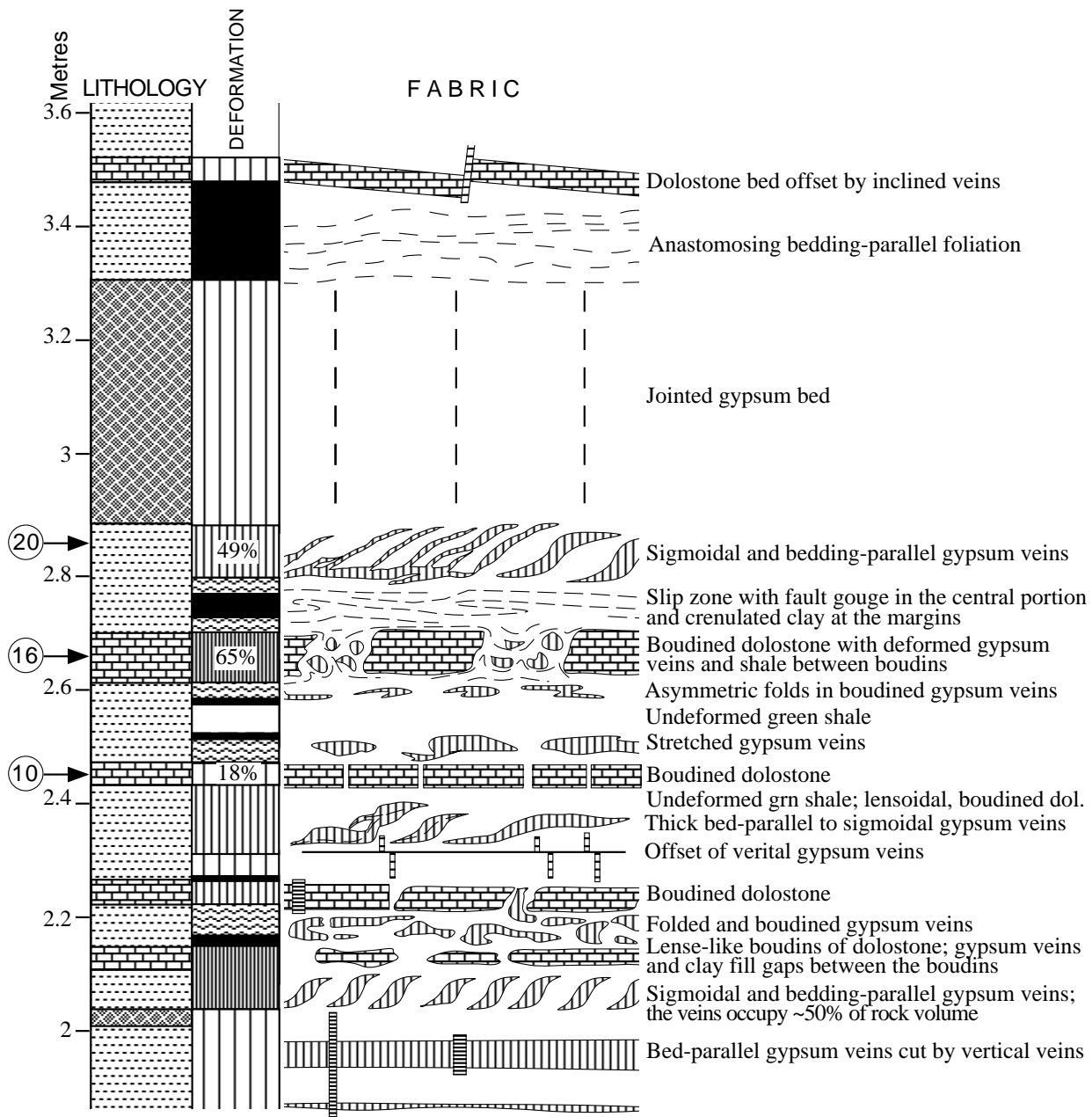


Figure 10. Enlargement of mechanical stratigraphy between 1.8 and 3.6 m. Arrows left of column indicate locations of mechanical units where extensional strain was measured.

Figure 11. Photograph of section between 2.24 and 2.84 m displaying the following deformation features. (A) Moderately (49%) extended shale with sigmoidal gypsum veins merging into common bed-parallel vein. (B) Slip and drag zones; vertical veins beneath abut against zones. (C) Slightly extended green shale with vertical gypsum veins. (D) Highly deformed drag zone with stretched and asymmetrically folded gypsum veins. (E) Highly (65%) extended dolostone; note flow of shale and deformed gypsum veins from adjacent drag zones into wide gaps between boudins. (F) Highly deformed drag zone with stretched and asymmetrically folded gypsum veins. (G) Slightly extended green shale with vertical gypsum veins. (H) Highly deformed drag zone with stretched and asymmetrically folded gypsum veins and floating hinges. (I) Slip zone. (J) Slightly extended green shale with vertical gypsum veins. (K) Slip zone. (L) Highly deformed drag zone with stretched and asymmetrically folded gypsum veins. (M) Slightly (18%) extended dolostone; note thin gaps between boudins filled with vertical gypsum veins and shale. (N) Moderately extended shale with sigmoidal gypsum veins merging into common bed-parallel vein. (O) Thin bed-parallel slip zone; note offset vertical gypsum veins. (P) Slightly extended green shale with vertical gypsum veins. (Q) Thin bed-parallel slip zone.

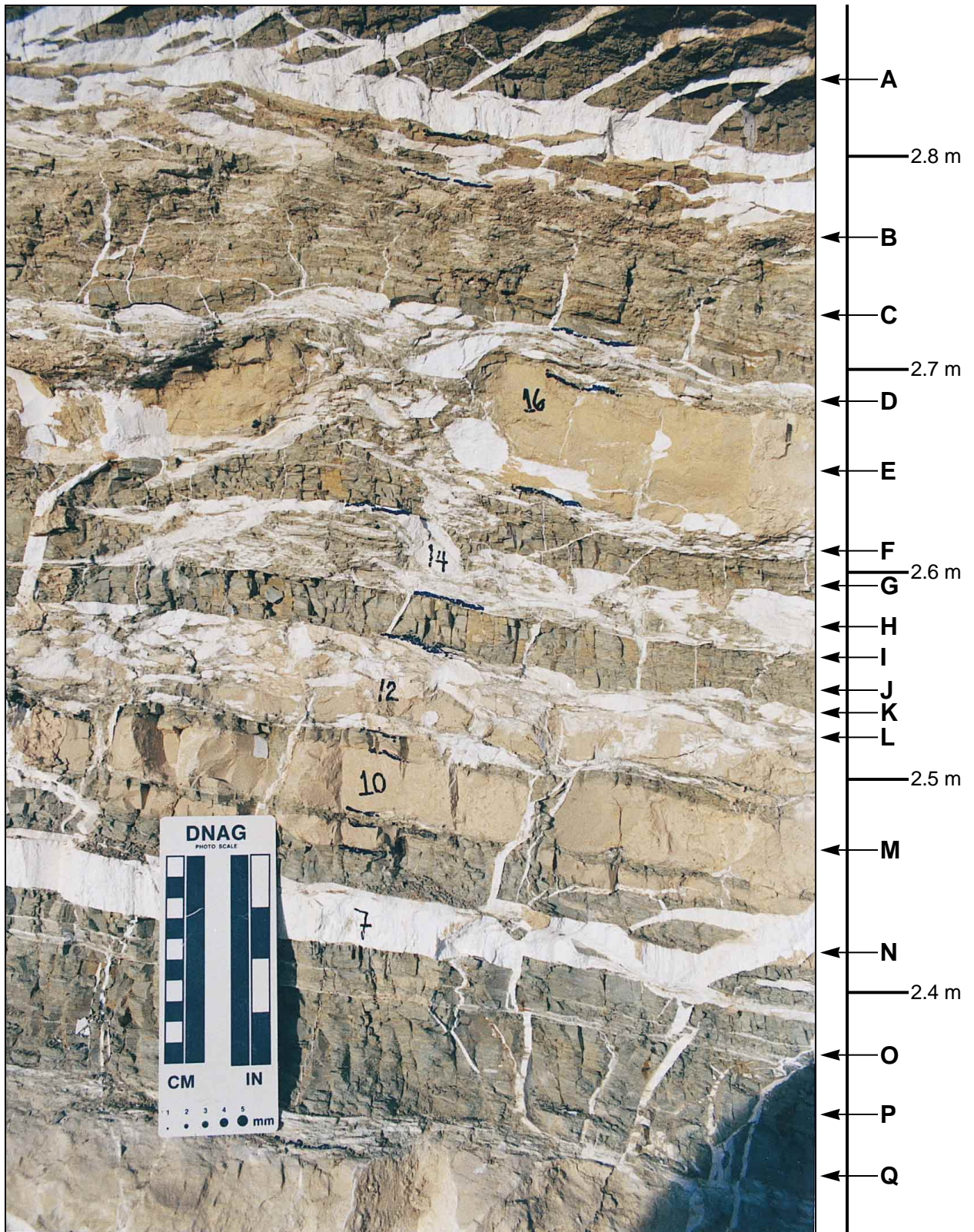


TABLE 1. EXTENSIONAL STRAIN CALCULATIONS FOR MECHANICAL UNITS AT MA'ALEH GEROFIT

Mechanical unit number	Height in section (m)	Structural element	Number of data	Scan line length (L^i) (cm)	ΔL (cm)	L^i (cm)	Strain ϵ (%)
1	1.30	Sigmoidal veins	37	4440.0	421.9	4018.0	10.5
10	2.45	Dolomite boudins	30	327.4	49.6	277.8	18
16	2.64	Dolomite boudins	8	268.5	105.5	163.0	65
20	2.81	Sigmoidal veins	23	145.0	47.7	97.3	49
29	4.89	Dolomite boudins	27	235.2	2.9	232.3	1.2

Note: Refer to Figure 9 for locations of units within the section.

Drag Zones

Deformed rocks adjacent to slip zones display evidence of frictional drag and hence are termed "drag zones." Drag zones are rich in gypsum that originated as bedding-parallel and sigmoidal veins. Due to friction, these veins were subsequently folded and stretched. Fold asymmetry provides a kinematic indicator for sense of slip, and the fact that backlimbs are boudined implies that asymmetric folding occurred in an overall extensional regime. As is the case for slip zones, zones of drag show evidence for expansion into neighboring layers. Drag zones may be present on both sides of a slip zone, as seen in the shale at approximately 2.7 m, or they may be found only on one side, as seen at 2.2 m (Fig. 10).

Extension Zones and Extensional Strain Measurements

One of the more striking aspects of the outcrop is the pervasive manifestation of extension, primarily in the form of opening-mode sigmoidal and bedding-parallel veins in shales and siltstones, as well as boudined carbonate layers (Fig. 11). Extensional strain was calculated for five mechanical units in the section that are well exposed, accessible, and display evidence of deformation in the form of sigmoidal veins and boudins (Table 1). All scan lines were performed parallel to bedding and trend approximately 114° in the plane containing both boudin and sigmoidal vein maximum stretch axes. For the dolostone layers we measured boudin and gap lengths, and for sigmoidal veins found in shale we measured vein apertures at their midpoints (Fig. 12). The extensional strain (ϵ) is defined as

$$\epsilon = \frac{\Delta L}{L^i} = \frac{\Delta L}{L^f - \Delta L}$$

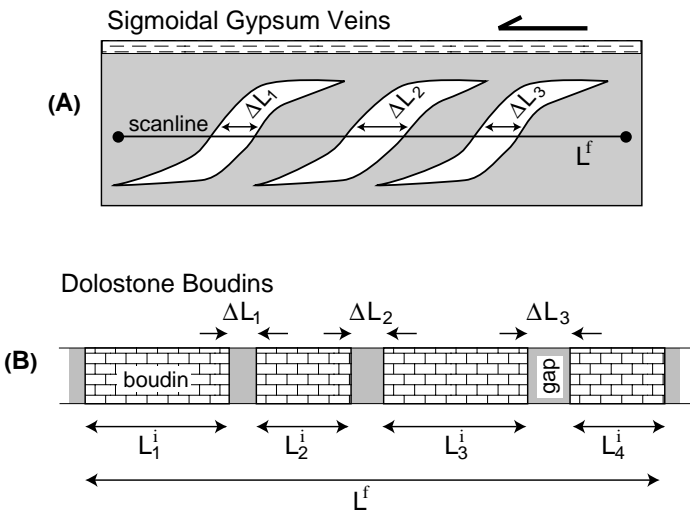


Figure 12. Methods of extensional strain measurement for sigmoidal veins in shale (A) and boudinaged dolostone beds (B). L refers to length. See text for more details.

where ΔL is the total change in length (i.e., $\Delta L = \Sigma \Delta L = \Delta L_1 + \Delta L_2 + \dots + \Delta L_n$), L^i equals the initial length (i.e., $L^i = \Sigma L^i = L^i_1 + L^i_2 + \dots + L^i_n$), and L^f is the final length. The amount of measured extension varies greatly, from 1.2% in unit 29 to 65% in unit 16.

Of particular interest are mechanical units 10, 16, and 20, found within the enlarged section of Figures 10 and 11 (i.e., between 1.8 and 3.6 m), because we attempt to calibrate relative strain magnitudes throughout the section according to these beds. Extension magnitudes are 18% for the 3.8-cm-thick boudined dolostone at 2.45 m, 65% for the 6.8-cm-thick boudined dolostone at 2.64 m, and 49% for the 6.7 cm shale cut by sigmoidal gypsum veins at 2.81 m (Table 1). We constructed a relative scale of extension magnitudes on the basis of these values, as shown in the legend of Figure 9; the scale was then assigned to each layer containing boudins or sigmoidal veins (Figs. 9 and 10). Beds without any evidence of extension are considered un-

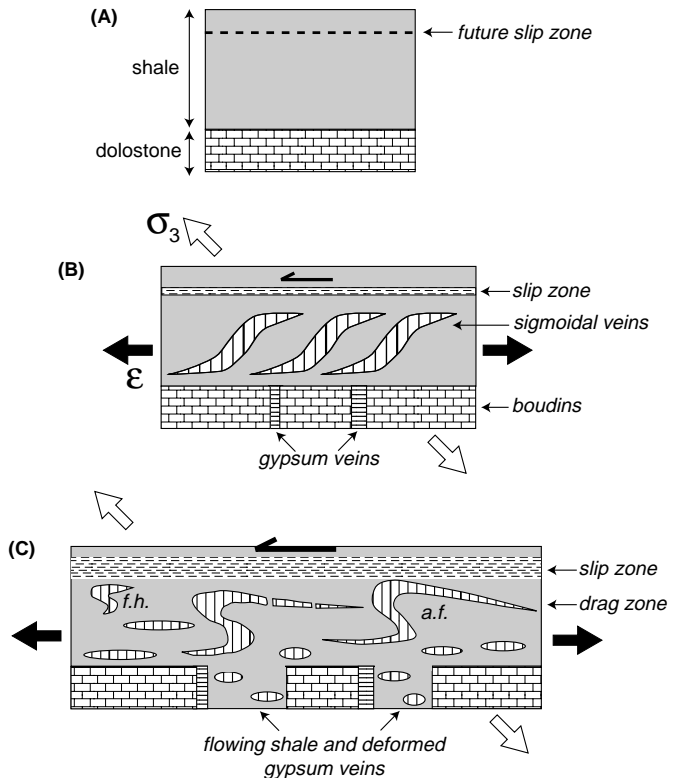


Figure 13. Sketch depicting development of extension and drag fabric features. (A) Zone of flexural slip develops in shale; (B) bedding-plane slip results in formation of sigmoidal veins in shale and boudins in carbonate rocks; (C) continued slip results in widening of slip zone, drag in adjacent shale, and increased extension. As a consequence, sigmoidal and bed-parallel gypsum veins fold and stretch, resulting in asymmetric folds (a.f.) and floating hinges (f.h.).

deformed. Beds that display extension similar to unit 10 (i.e., less than or equal to approximately 20%) are considered to have undergone a small amount of extension. Likewise, beds resembling mechanical unit 20 in terms of strain (about 50%) are assigned medium extension, whereas those beds displaying strain on a par with, or greater than mechanical unit 16 (greater than or equal to about 65%) are considered to have undergone large amounts of extension. As can be seen from plotting relative strain magnitudes (Figs. 9 and 10), extension varies considerably from one layer to the next throughout the section, with maximum extension found in beds directly in contact with slip horizons. The amount of extension decreases with increasing distance away from slip zones.

In our interpretation of the development of slip, extension, and drag zones, narrow bedding-plane slip zones nucleate in shale, which in turn results in the extension of neighboring beds (Fig. 13, A and B). Extension in shale is accommodated by sigmoidal veins, whereas boudinage takes place in dolostone; open spaces are filled with fibrous gypsum veins. Bedding-plane slip intensifies, further extending adjacent beds. Frictional drag in shale results in the deformation of sigmoidal gypsum veins, with asymmetrically folded veins and floating hinges serving as kinematic indicators within the drag zone (Fig. 13C). Deformed shale and gypsum veins flow into widened gaps between dolostone boudins.

Main Detachment and Deformation Zoning

The overall distribution and relative intensity of deformation in the section can be appreciated in light of the range of fabrics that developed in response to flexural slip, extension, and frictional drag. The 1-m-thick main detachment at the top of the measured section (10.8–11.8 m) represents the dominant flexural-slip horizon (Fig. 5B). Alternating planar and crenulated foliation characterize this dominantly shale detachment zone, which includes intensively crushed and boudined gypsum veins, fault gouge, and chaotic detachment folds. Zones of intense drag and boudinage in adjacent interbedded shale and limestone (10.3–10.8 m) attest to the significant amount of displacement accommodated by the main detachment.

In contrast to deformation associated with the main detachment and adjacent beds, large segments of the section remain relatively undeformed, such as the shale between 3.6 and 4.8 m, and the dolostone-gypsum horizons between 9.0 and 10.0 m. The variability in style and intensity of deformation is best seen in the enlarged section and accompanying photograph (Figs. 10 and 11). At 2 m the green shale and thin overlying gypsum bed are slightly deformed; bedding-parallel gypsum veins are cut by a later set of vertical gypsum veins. The abundance of gypsum-filled sigmoidal veins indicates that the green shale at approximately 2.08 m underwent a large amount of extension. Likewise, the wide gaps between overlying dolostone boudins imply a similar large amount of extension. Noncoincidentally, the base of the overlying shale (about 2.15 m) is a slip zone, itself overlain by a zone of drag. The dolostone at 2.24 m has been moderately extended through boudinage formation. The lithologically homogeneous shale between 2.3 and 2.42 m can be divided into four discrete zones of deformation; the lower part consists of slightly extended shale bounded above and below by thin slip horizons (note offset vertical veins in Fig. 11), whereas the upper part has been moderately extended by means of sigmoidal gypsum veins. Similar mechanical divisions are found within the shale occupying 2.46–2.61 m in the section; drag zones are characterized by asymmetric folds flanking slip horizons. The approximately 65% dolostone extension at 2.63 m resulted in the flowing of shale and deformed gypsum veins into boudin gaps (Fig. 11). This highly extended dolostone bed is situated between a series of drag and slip zones in adjacent shale. The slip zone at 3.4 m is situated above a slightly deformed jointed gypsum bed and beneath a slightly deformed dolostone.

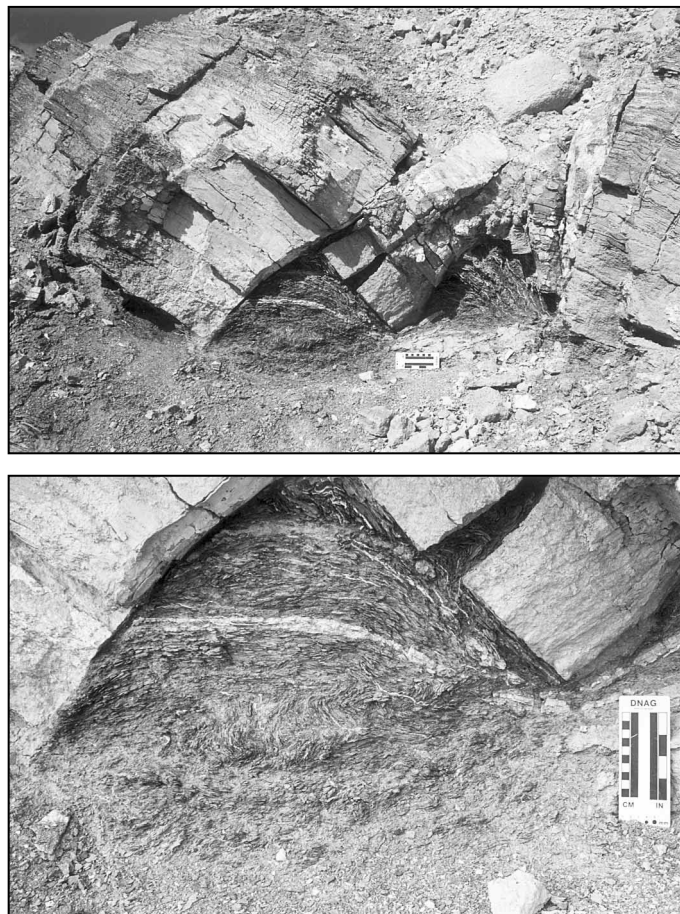


Figure 14. (A) Antithetically rotated gypsum blocks (about 9.5 m in section) resulting from top-to-the-west simple shear, with shale flowing into “triangle zones”; (B) close-up of triangle zone with chaotically folded shale and gypsum veins. Note the development of top-to-the-east asymmetric folds due to local shear couples developed in triangle zone.

In addition to the heterogeneous distribution of deformation style and intensity, another important observation is the dip direction of sigmoidal veins. East-dipping sigmoids, implying top-to-the-east flexural slip, are found in the section at 6.8, 7, 7.8, and 8.8 m. These sigmoids are not very prominent; they display small apertures that correspond to extensional strains of less than 1%–3%. In contrast, west-dipping sigmoidal veins, which are found at 1.3, 2.1, 2.35, 2.85, 4.9, and 5.5 m, have much greater apertures and account for large amounts of extension (Table 1).

ANTITHETIC BLOCK ROTATION

Having described relationships between fabric development and mechanical stratigraphy, we now focus on the other major structural aspect of the Ma’aleh Gerofit outcrop: fault-bounded blocks at different scales that have been tilted by rotation about a horizontal axis. As shown in the stereogram (Fig. 8), the overwhelming majority of normal faults are west-dipping, resulting in a consistent clockwise block rotation around a north-pointing horizontal axis. An antithetic origin due to top-to-the-west simple shear is highly plausible in light of the pervasive syn-rotation extension as well as fibrous vein fill between blocks (Jordan, 1991; Fig. 2).

The largest faults displace the entire section up to about 10.5 m, where they are bounded above by the main detachment. The base of these large rotated blocks is not exposed, although maximum displacement across the central fault in Figure 5 is 9.6 m. Rollover in the hanging wall along with dragged beds in both the footwall and hanging wall are common features associated with this group of large faults (Fig. 4). In contrast, the smallest rotated blocks involve single beds of dolostone or gypsum, where a preexisting set of bed-normal joints serves as slip planes that accommodated block rotation (Fig. 14). Examples of block rotation confined to discrete beds are found at 3 m in a gypsum bed, at 6.1 m in a fossiliferous carbonate bed, and at 9.5 m in a gypsum bed. In all cases block rotation is facilitated by slip zones in bounding shale, and the sense of rotation in individual beds is similar to that of large blocks that span the entire section height. Narrow slip zones in the form of bedding-parallel gypsum veins commonly terminate against corners of rotated blocks that protrude into neighboring shale. In cases where block rotation is more advanced, such as shown in Figure 14, shale flowed freely into triangular gaps that developed between rotating blocks. These "triangle zones" are characterized by chaotically folded shale and veins along with boudined and thrust dolostone beds. Rotated blocks of intermediate size span the interval between 3.3 and 6.4 m in the section. This approximately 3.1-m-thick sequence of shale, siltstone, and carbonate beds is divided into a series of rotated blocks by steeply dipping, gypsum-

filled normal faults (Fig. 15). Note that the positions of major slip zones coincide exactly with the boundaries of rotated blocks.

DISCUSSION

The unique combination of flexural slip, fabric development, and block rotation observed at the Ma'aleh Gerofit outcrop must fit in mechanically with the overall bulk extension that predominates both locally as a result of monoclinial flexure above a basement normal fault, and regionally with respect to rifting along the margins of the Dead Sea transform (Garfunkel, 1981; Eyal et al., 1981; Eyal and Reches, 1983; Picard, 1987). In the following section we provide models to explain the relation between differential extension and flexural slip, as well as the progressive development of block rotations at different scales.

Variations in Extension Due to Nonuniform Slip Distribution

Four important observations provide limitations on the development of extensional structures in the Ma'aleh Gerofit outcrop. First, extension predominates throughout the section and is manifested in many ways such as sigmoidal veins, boudinage, and stretched backlimbs of drag folds. Second, extension varies a great deal throughout the section, and is as much as 65% in some beds. However, extension magnitude is not randomly distributed; maximum extension commonly occurs adjacent to slip horizons, whereas beds displaying minimum to zero extension are farther away from slip zones. Third, extensional fabrics are directly linked to simple shear along bedding planes, which in turn results from the flexural-slip mechanism. Fourth, slip zones vary in terms of intensity of deformation, thickness, and thickness of adjacent drag zones. Intensity of slip, in turn, appears to affect extension magnitudes in neighboring beds. A model describing the development of extensional structures must therefore take into account the correlation between extension magnitude and distribution and relative intensity of bedding-plane slip zones.

For the case where flexural slip is distributed uniformly across bedding planes of equal cohesion, slip vectors are of the same magnitude throughout the section, resulting in uniform displacement across the interfaces and the preservation of individual bed lengths (Fig. 16A). In the event that slip is concentrated along several major horizons of low cohesion, however, as is the case at Ma'aleh Gerofit, displacement gradients will develop. Major bedding-plane slip zones are akin to ductile shear zones, where displacement decreases in magnitude with increasing distance away from the shear zone (Ramsay and Huber, 1987). Therefore, displacement vectors will differ in magnitude between the top and bottom of individual beds, and the difference between these vectors may result in extension of that bed (Fig. 16B). The amount of extension, depicted as the difference between bed-boundary-slip vectors applied to the middle of each bed, will mirror displacement gradients between slip zones. Consequently, maximum displacement will occur in beds adjacent to major slip zones, and decrease to a minimum away from the zone. Variations in frictional properties and layer thicknesses will result in a more complex, asymmetric displacement profile, although the general relationship will remain.

Extension observed in the Ma'aleh Gerofit section follows the general pattern depicted in Figure 16B. Focusing on the section between 2.0 and 2.85 m, highly extended beds such as the dolostone at 2.15 m and 2.64 m are situated adjacent to relatively thick slip zones, whereas the dolostone at 2.45 m next to a thin slip zone displays only 18% extension (Figs. 10 and 11). The same relationship is found within the rotated sequence of beds between 3.3 and 6.4 m; almost no extension is found in the carbonate at 4.3 m, and small to medium extension is observed in carbonates adjacent to the slip zone at 6.4 m (Fig. 9).

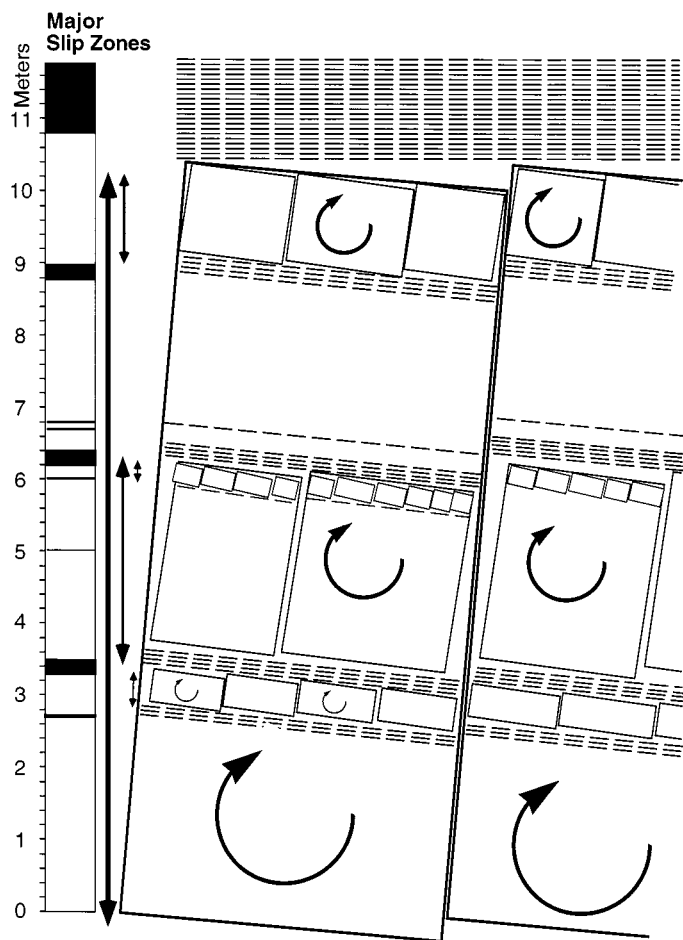


Figure 15. Block rotations at different scales observed at Ma'aleh Gerofit. Arrow height equals the height of rotated blocks. Note that major slip zones are located precisely above and beneath zones of block rotation, because they accommodate flexural slip when slip zones within rotating blocks become inactive.

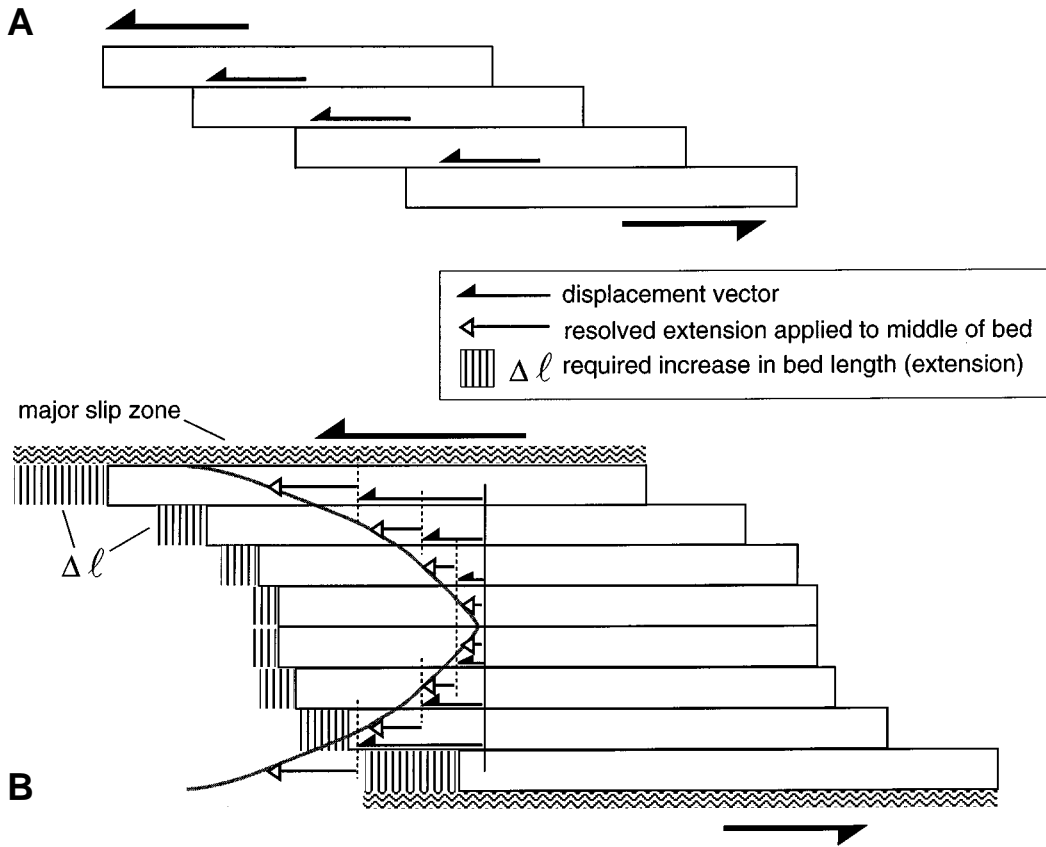
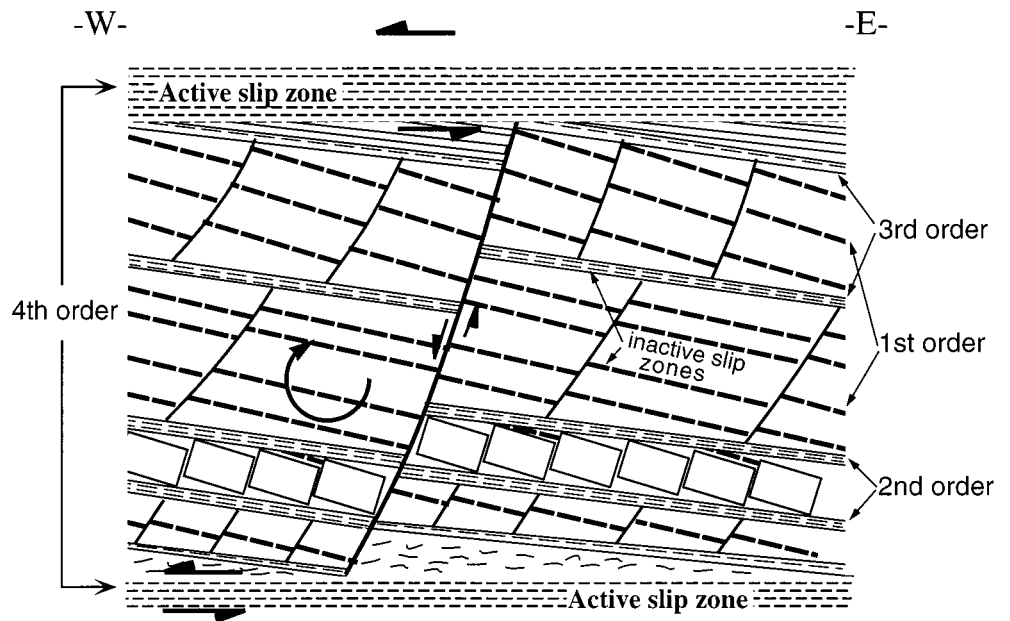


Figure 16. Model explaining the relationship between flexural slip and variations in relative extension observed in the section. (A) Flexural slip distributed evenly across all bed boundaries does not require changes in bed lengths; (B) variations in cohesion along bed boundaries results in nonuniform-slip distribution, and the amount of slip will decrease in magnitude away from major slip zones. The difference between slip vectors at the top and bottom of a bed creates extension in that bed. Variations in bed thickness and frictional properties will result in a more complex strain pattern.

Figure 17. Schematic diagram of the relation between block rotations and flexural-slip zones. Slip along first-order zones is distributed throughout the section, eventually resulting in block rotation within individual beds. Block rotation, in turn, renders several first-order zones inactive, resulting in the formation of second-order zones above and below rotating blocks. The trend toward larger blocks and more widely spaced slip zones continues in this manner.



Transfer of Bedding-Plane Slip Due to Block Rotation

Several key observations lead to the conclusion that block rotation and the progressive development of slip zones, ultimately leading to the creation of the main detachment, are closely linked. First, thin (0.5–1 cm thick), less-

developed slip zones abut against edges of rotated blocks, indicating that they no longer serve as active zones for flexural slip. Second, block height corresponds precisely to the stratigraphic spacing found between minor, intermediate, and major slip zones. Third, widths of block-bounding slip zones increase with increasing block size, implying that flexural slip be-

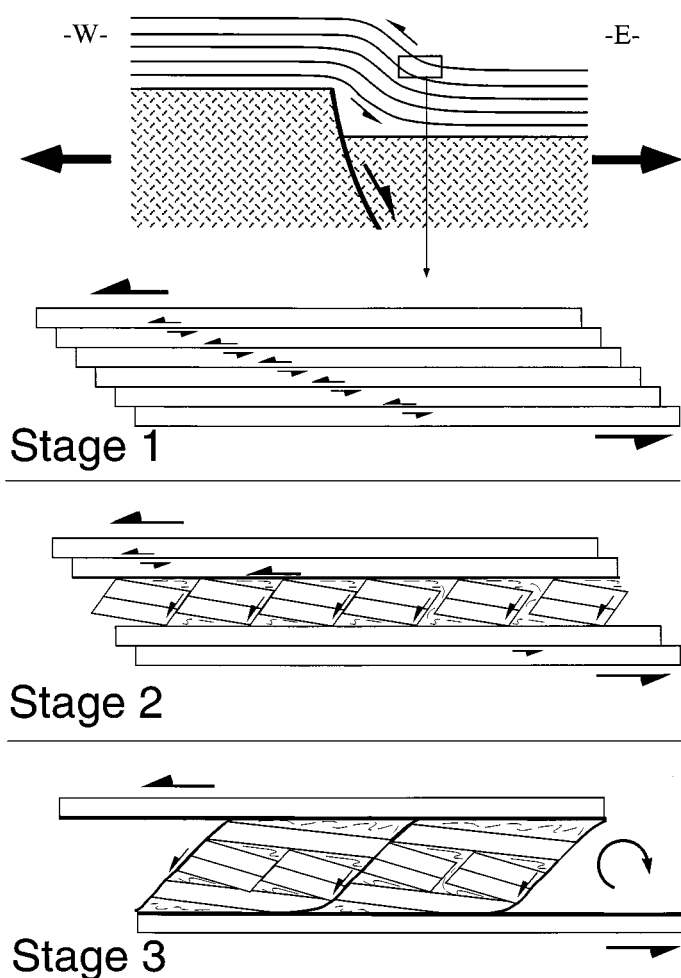


Figure 18. General model for development of flexural slip and block rotations at the Ma'aleh Gerofit section.

comes concentrated in fewer larger slip zones as rotated block size increases. Fourth, as shown in the column of mechanical stratigraphy (Fig. 9), the intensity of deformation varies dramatically within the section, implying that while some sequences of beds continued to undergo flexural slip and hence fabric development, in other parts of the section bedding-parallel slip terminated at a much earlier stage.

Bedding-plane slip due to flexural slip was initially distributed across numerous thin slip zones throughout the section (labeled "first-order" slip zones in Fig. 17). At this stage rock type was the deciding factor for slip distribution, and slip occurred exclusively in shale and siltstone. The continuation of top-to-the-west flexural slip parallel to bedding led to block rotation within individual beds, with a clockwise sense of rotation when viewed to the north. Block rotation in individual beds, in turn, led to the termination of active slip along those first-order zones that abutted against block edges protruding into adjacent shale (Fig. 17). Thus, flexural slip could no longer be accommodated within individual rotated blocks, and slip was transferred to second-order zones situated directly above and beneath the bed of rotating blocks. At this point the dimensions of rotating blocks began to act as an additional control on the location of slip zones in the section. The process of transfer and concentration of slip into fewer horizons continued as block size increased to incorporate sequences of beds, with the development of

intermediate-size rotated blocks bounded by third-order slip zones, and ultimately the large blocks ≥ 10.2 m bounded above by the main detachment zone (fourth-order slip zone). In this manner rigid block rotation due to bedding-plane slip provided the mechanism for transferring displacement from multiple bed-parallel horizons to several widely spaced major detachments.

Rotation of individual and small groups of beds did not necessarily occur at the same time, which may explain the dramatic differences in fabric intensity among different parts of the section. For example, slip, extension, and drag zones are considerably more developed in the interval between 2.0 and 2.9 m when compared with similar rocks between 3.6 and 6.2 m. Thus, rotation of the block between 3.3 and 6.4 m occurred relatively early, locking internal slip zones and effectively preventing the continued development of internal fabric. On the other hand, slip along discrete horizons between 2.0 and 2.9 m continued up until the entire sequence of blocks ≥ 10.2 m began to rotate (i.e., at a much later stage), thereby resulting in extensive development of sigmoidal veins and boudins within this interval.

Mesostructures and fabrics observed at Ma'aleh Gerofit provide the information needed to develop a model for the progressive development of flexural slip within the regional context of an extensional drape fold (Fig. 18). Flexural slip in the Ora Formation occurred in response to a monoclinial drape fold that developed above the hanging wall of a down-dropped basement block. This resulted in an overall top-to-the-west flexural slip that was distributed across numerous slip horizons within the Ora shale (stage 1). As flexural slip progressed, rigid blocks of individual beds and small sequences of beds rotated, resulting in the formation of antithetically rotated pull-aparts (stage 2). In the process, slip terminated across individual zones within the rotated blocks and was transferred to wider block-bounding slip horizons. Eventually large normal faults propagated across the entire section (≥ 10.2 m thick), creating large rotated blocks bounded by major detachments (stage 3). At a later stage, the basement-offsetting normal fault propagated through the overlying strata, creating a rollover anticline (Fig. 3). Top-to-the-east flexural slip due to this later structure resulted in the growth of east-dipping sigmoidal veins, although the extent of their development was limited by the preexisting system of rotated blocks.

CONCLUSIONS

Flexural slip occurred in incompetent shale of the Ora Formation while sedimentary cover draped into a monoclinial structure above a basement-bounding normal fault at the western margin of the Dead Sea rift. The combination of flexural slip and regional extension resulted in a unique set of mesoscopic fabrics; extension is manifested in the formation of boudinage and fibrous gypsum veins, whereas intense foliation and drag folds attest to a significant component of bedding-plane slip. Intensity of fabric development varies dramatically within the section, corresponding directly to intensity of localized bedding-plane slip. Kinematic indicators show a dominant top-to-the-west sense of motion, consistent with the expected sense of flexural slip for the regional monoclinial structure.

Simple shear parallel to bedding ultimately led to antithetic block rotation within competent beds, which in turn controlled the position of active slip planes. Bedding-plane slip was initially distributed across many narrow zones throughout the Ora Formation. However, when these slip zones terminated against block-bounding faults they became inactive, transferring active slip to wider zones above and beneath mechanically confined rotating blocks. Spacing between active-slip horizons increased with increasing block size, and in this manner flexural slip in the Ora Formation became concentrated along several major detachments. Thus, the wide variability in intensity of fabric development in the Ora Formation may be attributed to variations in magnitude of flexural slip, which in turn is controlled by the timing and location of rotating blocks.

ACKNOWLEDGMENTS

Funding for this project was provided in part by grants from the Florida International University Foundation, NATO Collaborative Research grant 951350, and Direcccion General de Investigación Científica y Técnica project PB93-1149 CO3-CO2. We are grateful to Diane Pirie and Salamanca University for thin-section preparation, and the Ramon Science Center and Leon Pancirer for logistical support and use of facilities. Reviews by Amos Nur, Arthur Sylvester, Bob Bohannon, and John Geissman are sincerely appreciated.

REFERENCES CITED

- Alonso, J. L., 1989, Fold reactivation involving angular unconformable sequences: Theoretical analysis and natural examples from the Cantabrian Zone (Northwestern Spain): *Tectonophysics*, v. 170, p. 57–77.
- Arkin, Y., 1989, Large-scale tensional features along the Dead Sea–Jordan Rift Valley: *Tectonophysics*, v. 165, p. 143–154.
- Bartov, J., Eyal, Y., Garfunkel, Z., and Steinitz, G., 1972, Late Cretaceous and Tertiary stratigraphy and paleogeography of southern Israel: *Israel Journal of Earth Sciences*, v. 21, p. 69–97.
- Becker, A., Mazor, E., and Becker, N., 1995, Flexural slip in an anticlinal plungeout as a mechanism for dike offsets: Nahal Ardon Valley, Ramon National Geological Park, Israel: *International Geology Review*, v. 37, p. 601–622.
- Behzadi, H., and Dubey, A. K., 1980, Variation of interlayer slip in space and time during flexural slip folding: *Journal of Structural Geology*, v. 2, p. 453–457.
- Chapple, W. M., and Spang, J. H., 1974, Significance of layer-parallel slip during folding of layered sedimentary rocks: *Geological Society of America Bulletin*, v. 85, p. 1523–1534.
- Etheridge, M. A., Branson, J. C., and Stuart-Smith, P. G., 1985, Extensional basin-forming structures in Bass Strait and their importance for hydrocarbon exploration: *Australian Petroleum Exploration Association Journal*, v. 25, p. 344–361.
- Eyal, M., Eyal, Y., Bartov, Y., and Steinitz, G., 1981, The tectonic development of the western margin of the Gulf of Elat Rift: *Tectonophysics*, v. 80, p. 39–60.
- Eyal, Y., 1973, The tectonics of the Shelomo and Yotam grabens, Eilat, Israel: *Israel Journal of Earth Sciences*, v. 22, p. 165–184.
- Eyal, Y., and Rechess, Z., 1983, Tectonic analysis of the Dead Sea rift region since the Late Cretaceous based on mesostructures: *Tectonics*, v. 2, p. 167–185.
- Garfunkel, Z., 1981, Internal structure of the Dead Sea leaky transform (rift) in relation to plate kinematics: *Tectonophysics*, v. 80, p. 81–108.
- Garfunkel, Z., Zak, I., and Freund, R., 1981, Active faulting along the Dead Sea transform (rift): *Tectonophysics*, v. 80, p. 1–26.
- Gaudemer, Y., and Tapponier, P., 1987, Ductile and brittle deformations in the northern Snake Range, Nevada: *Journal of Structural Geology*, v. 9, p. 159–180.
- Gibbs, A. D., 1987, Development of extension and mixed-mode sedimentary basins, in Coward, M. P., Dewey, J. F., and Hancock, P. L., eds., *Continental extensional tectonics*: Geological Society [London] Special Publication 28, p. 19–33.
- Ginat, H., 1995, The geology and geomorphology of Yotveta region [Master's thesis]: Jerusalem, Israel, Hebrew University, 71 p.
- Goldstein, A. G., 1988, Factors affecting the kinematic interpretation of asymmetric boudinage in shear zones: *Journal of Structural Geology*, v. 10, p. 707–715.
- Gross, M. R., 1995, Fracture partitioning: Failure mode as a function of lithology in the Monterey Formation of coastal California: *Geological Society of America Bulletin*, v. 107, p. 779–792.
- Hanmer, S. K., 1982, Vein arrays as kinematic indicators in kinked anisotropic materials: *Journal of Structural Geology*, v. 4, p. 151–160.
- Hanmer, S., 1986, Asymmetrical pull-aparts and foliation fish as kinematic indicators: *Journal of Structural Geology*, v. 8, p. 111–122.
- Jackson, J. A., and McKenzie, D. P., 1983, The geometrical evolution of normal fault systems: *Journal of Structural Geology*, v. 5, p. 471–482.
- Jackson, J. A., White, N. J., Garfunkel, Z., and Anderson, H., 1988, Relations between normal-fault geometry, tilting and vertical motions in extensional terrains: An example from the southern Gulf of Suez: *Journal of Structural Geology*, v. 10, p. 155–170.
- Jordan, P. G., 1991, Development of asymmetric shale pull-aparts in evaporite shear zones: *Journal of Structural Geology*, v. 13, p. 399–409.
- Lewy, Z., 1988, Lithostratigraphic subdivision of Hazera Formation (late Albian–late Cenomanian) in the Negev, southern Israel: *Israel Journal of Earth Sciences*, v. 37, p. 205–210.
- Lister, G. S., Etheridge, M. A., and Symonds, P. A., 1986, Detachment faulting and the evolution of passive continental margins: *Geology*, v. 14, p. 246–250.
- Malavieille, J., 1987, Kinematics of compressional and extensional ductile shearing deformation in a metamorphic core complex of the northeastern Basin and Range: *Journal of Structural Geology*, v. 9, p. 541–554.
- Marcoux, J., Brun, J.-P., Burg, J.-P., and Ricou, L. E., 1987, Shear structures in anhydrite at the base of thrust sheets (Antalya, southern Turkey): *Journal of Structural Geology*, v. 9, p. 555–561.
- Picard, L., 1987, The Elat (Aqaba)–Dead Sea–Jordan subgraben system: *Tectonophysics*, v. 141, p. 23–32.
- Platt, J. P., 1979, Extensional crenulation cleavage: *Journal of Structural Geology*, v. 1, p. 95–96.
- Platt, J. P., 1984, Secondary cleavages in ductile shear zones: *Journal of Structural Geology*, v. 6, p. 439–442.
- Platt, J. P., and Vissers, R. L. M., 1980, Extensional structures in anisotropic rocks: *Journal of Structural Geology*, v. 2, p. 397–410.
- Quennell, A. M., 1959, Tectonics of the Dead Sea rift: *International Geological Congress*, 20th, p. 385–405.
- Ramberg, H., 1955, Natural and experimental boudinage and pinch and swell structure: *Journal of Geology*, v. 63, p. 512–526.
- Ramsay, J. G., 1967, *Folding and fracturing of rocks*: New York, McGraw-Hill, 568 p.
- Ramsay, J. G., 1974, Development of chevron folds: *Geological Society of America Bulletin*, v. 85, p. 1741–1754.
- Ramsay, J. G., and Huber, M. I., 1987, *The techniques of modern structural geology*: London, United Kingdom, Academic Press, 700 p.
- Roberts, A., and Yielding, G., 1994, Continental extensional tectonics, in Hancock, P. L., ed., *Continental deformation*: Oxford, United Kingdom, Pergamon, p. 223–250.
- Schlische, R. W., 1995, Geometry and origin of fault-related folds in extensional settings: *American Association of Petroleum Geologists Bulletin*, v. 79, p. 1661–1678.
- Stearns, D. W., 1978, Faulting and forced folding in the Rocky Mountain foreland, in Matthews, V., III, ed., *Laramide folding associated with basement block faulting in the western United States*: Geological Society of America Memoir 151, p. 1–37.
- Stock, P., 1992, A strain model for antithetic fabric rotation in shear band structures: *Journal of Structural Geology*, v. 14, p. 1267–1275.
- Stone, D. S., 1993, Basement-involved thrust-generated folds as seismically imaged in the subsurface of the central Rocky Mountain foreland, in Schmidt, C. Chase, R. B., and Erslev, E. A., eds., *Laramide basement deformation in the Rocky Mountain foreland of the western United States*: Geological Society of America Special Paper 280, p. 271–318.
- Suppe, J., 1985, *Principles of structural geology*: Englewood Cliffs, New Jersey, Prentice-Hall, 537 p.
- Tanner, P. W. G., 1989, The flexural-slip mechanism: *Journal of Structural Geology*, v. 11, p. 635–655.
- Tanner, P. W. G., 1992, Morphology and geometry of duplexes formed during flexural-slip folding: *Journal of Structural Geology*, v. 14, p. 1173–1192.
- Wernicke, B., and Burchfiel, B. C., 1982, Modes of extensional tectonics: *Journal of Structural Geology*, v. 4, p. 105–115.
- Zak, I., and Freund, R., 1966, Recent strike-slip movements along the Dead Sea rift: *Israel Journal of Earth Sciences*, v. 15, p. 33–37.

MANUSCRIPT RECEIVED BY THE SOCIETY JANUARY 25, 1996

REVISED MANUSCRIPT RECEIVED NOVEMBER 24, 1996

MANUSCRIPT ACCEPTED JANUARY 11, 1997